ISSN 2221-8688

THERMODYNAMIC STUDY OF COPPER ARSENIDES BY THE EMF METHOD WITH THE Cu₄RbCl₃I₂ SOLID ELECTROLYTE

^{1,2} D.M. Babanly, ^{1*}A.R. Aghayeva, ³ E.N. Orujlu, ⁴G.B. Dashdiyeva, ² E.J. Ahmadov, ² D.B. Tagiyev

¹ French - Azerbaijani University, Azerbaijan State Oil and Industry University (ASOIU), Nizami 183, Baku, Azerbaijan

² Institute of Catalysis and Inorganic Chemistry (ICIC), H. Javid 113, Baku, Azerbaijan ³ Azerbaijan State Oil and Industry University (ASOIU), Azadlig 20, Baku, Azerbaijan ⁴ Baku Engineering University (BEU), H. Aliyev 120, Baku, Azerbaijan ^{*}e-mail: aytekin agayeva@mail.ru

Received 18.10.2024 Accepted 28.12.2024

Abstract. The present work demonstrates the thermodynamic study of copper arsenides using electromotive force measurements with a solid Cu⁺ conductive electrolyte, Cu₄RbCl₃I₂, within the temperature range of 300–440 K. Measurements were performed using the equilibrium samples from the Cu₃As + As, Cu₃As + Cu₈As, and Cu₈As + (Cu) two-phase regions of the Cu-As system. The phase compositions of all samples were controlled using the powder X-ray diffraction method. The partial molar functions of copper in alloys, as well as the standard thermodynamic functions of formation and standard entropies of the Cu₃As, Cu₈As compounds, as well as, the Cu_{0.94}As_{0.06} solid solutions based on copper, were calculated. A thermodynamic study of the Cu₈As compound and the Cu_{0.94}As_{0.06} solid solution has been carried out for the first time in the current contribution. Thermodynamic properties for the Cu₃As compound obtained in this work have been analyzed compared with the available literature data.

Keywords: Cu_3As compound; Cu_8As compound; $Cu_{0.94}As_{0.06}$ solid solutions, emf measurements, thermodynamic functions.

DOI: 10.32737/2221-8688-2025-3-375-387

1. Introduction

Arsenides play a crucial role in developing advanced technologies, such as semiconductors for electronics, thermoelectric devices for energy conversion, and specialized alloys for industrial applications. Additionally, arsenides are of interest in metallurgy and geochemistry, as they frequently occur in natural ores and influence the extraction and processing of valuable metals [1-3].

Metal arsenides exhibit unique combination of electronic, optical, and physical properties, making them highly valuable for a range of advanced technological broad applications, despite their inherent toxicity [4-6]. Many of these compounds function as semiconductors with direct band gaps, which makes them particularly advantageous for optoelectronics, including laser diodes, and highefficiency solar cells [7-10].Beyond optoelectronics, metal arsenides play a crucial

role in high-speed electronics, where their excellent charge carrier mobility enables the development of ultra-fast transistors communication systems. Furthermore, their role in spintronic is gaining attention, as certain metal arsenides exhibit spin-polarized electronic states that can be exploited for low-power, highefficiency data storage and processing. Their widespread applicability across disciplines, from telecommunications defense systems to medical imaging renewable energy, underscores the importance of continued research into their properties, and potential modifications to mitigate toxicity while enhancing performance [11-15].

The Cu-As system is vital to both the copper and lead industries. Understanding the behavior of arsenic in liquid phases is critical for predicting its distribution across slag, matte, liquid copper, and gas phases during the

pyrometallurgical extraction of copper. In the smelting of complex lead-copper materials, a multicomponent liquid speiss enriched with Cu and As can form. The presence of arsenic in lead bullion significantly affects the decoppering process due to the formation of solid copper arsenide [16-18].

Copper arsenides possess unique electronic properties and have the potential for applications in thermoelectric devices. Additionally, their catalytic properties are being studied for possible use in various chemical reactions. Furthermore, the Cu-As system serves as an important reference for activity measurements in related systems, such as Cu-As-S(Pb). As a result, an accurate thermodynamic characterization of this system is essential for correctly interpreting experimental data in more complex, higher-order systems [19]. Understanding its thermodynamic behavior is essential for optimizing the extraction of copper and arsenic from ores and for modeling the evolution of mineral assemblages in geological environments.

Extensive studies have been conducted on the phase relationships in the Cu-As system. Hansen [20] and Elliott [21] identified several phases and reactions, including the terminal solid solution (Cu), which exhibits a broad solubility range; congruently melting Cu₃As, in eutectic equilibrium with (Cu); a high-temperature compound, tentatively identified as Cu₅As₂, which forms peritectically from the liquid and Cu₃As, and later decomposes eutectoidally into Cu₃As and an As-rich phase; and the eutectic reaction between Cu₅As₂ and an As-rich phase of unknown composition. The stoichiometry of the most Cu-rich compound was given as Cu₉As, Cu₈As, Cu₇As and Cu₆As by different authors. Cu₅As₂ was subsequently designated Cu₁₉As₈ by [22]. The phase diagram proposed by [23] shows the existence of two additional compounds, Cu₁₅As₄ and Cu₂As.

Subramanian and Laughlin [24] conducted a review of available experimental data on phase equilibria in 1988 and proposed the equilibrium diagram for the Cu-As system which follows the essential features of [20, 21], with certain revisions based on more recent experimental investigations. The phases accepted in [24] are: the liquid phase - L; the face-centered cubic (fcc) terminal solid solution based on copper with a maximum solid solubility of 6.83 at.% As at the

eutectic temperature of 958K; the copper-rich cubic close-packed (cph) β phase (A3, Mg type), forming peritectoidally from (Cu) and γ / phases at 598K; hexagonal γ-phase (D0₁₈, Na₃As type) forming congruently from the liquid at 26.25 at.% As and 1100K; hexagonal γ' phase (Cu₃As type), existing over the 25.5 to 27.8 at.% As composition range and undergoing an allotropic hexagonal transformation to γ-phase temperatures between 723 and 748 K; cubic δ phase (D03, BiF2 type), forming peritectically from L and γ-phases at 982 K and 29 at.% As composition and undergoing an allotropic transformation to orthorhombic δ' at 653K; orthorhombic δ'-phase (Cu₅As₂ type), existing over the limited temperature range 573 to 653K and decomposing eutectoidally into γ' and $\alpha(As)$ phases at 573 K and 29 at.% As; and pure (α -As) and (\varepsilon-As) phases with no reported solid solubility of copper [24].

Further study was conducted by Teppo and Taskinen [25], who included additional results in the phase diagram dataset and conducted a thermodynamic assessment. In that assessment [25], the phase diagram and activity data were evaluated simultaneously using the least squares method. The phase diagram was well described by the produced set of model parameters and there were not considerable differences with the diagram given in [24].

The last, more advanced thermodynamic assessment of the Cu-As system was conducted by the implementation of the Calphad-type optimization in [26] in 2018. Calculations of the study were performed using FactSage 7.0 software and a comparison with earlier work of [25] was given throughout in that paper. All relevant information including phase equilibria data, activities, heat capacities, heats of mixing heat of formation evaluated and are thermodynamically simultaneously in a consistent way to produce one set of model equations for the Gibbs energies of all phases in [26]. The phase diagram of the Cu-As system described in [26] is given in Fig.1. Thin red lines are adapted from the assessment of [24]. Thin blue lines are calculated using model parameters of Teppo and Taskinen [25]. Thick black lines are calculated using model parameters in [26]. Symbols are experimental data taken from different studies.

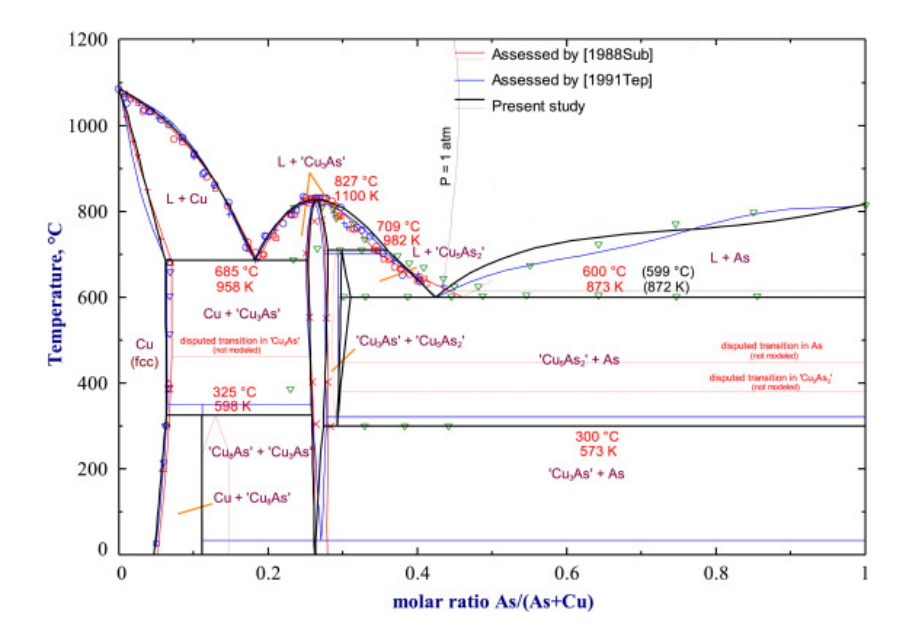


Fig. 1. Phase diagram of the Cu-As system [26]

The *emf* method, along with its different adaptations, is widely used thermodynamic analysis of both binary and more complex inorganic systems. The selection of an electrolyte for the emf method is influenced by several key factors. including chemical compatibility with the electrodes, nonwith reaction, interference the stability, temperature range, and ionic species, among others, to ensure precise measurements [27-34].

The traditional application of the emf method with liquid electrolytes in coppercontaining systems is limited by difficulties in maintaining a stable charge of copper ions (+1) in the electrolyte, as well as the presence of less noble metals than copper [35]. However, studies have shown that cation-conducting electrolytes can be effectively employed for the thermodynamic analysis of copper-containing compounds using the emf method, even when these electrolytes include metals that are less noble than copper [36-39]. For instance, the

Cu₄RbCl₃I₂ electrolyte demonstrates high and nearly pure ion conductivity for Cu⁺ cations at room temperature [39, 40]. These characteristics make Cu₄RbCl₃I₂ particularly suitable for the thermodynamic investigation of various coppercontaining compounds [41-46].

Thermodynamic properties of the Cu₃As compound have been studied in several works and summarized in modern reviews and databases. Analysis shows that the results of those works are highly scattered. Moreover, there is no available literature data about the thermodynamic study of the other copper arsenides. Therefore, to achieve a more reliable set of thermodynamic functions on Cu₃As compound and to study thermodynamic properties of other copper arsenides, this work focuses on the thermodynamic study of copper arsenides using the emf method with the solid Cu⁺ conductive electrolyte, Cu₄RbCl₃I₂, within the temperature range of 300–440 K.

2. Experimental part

The compositions of the prepared samples, along with their synthesis and thermal annealing conditions, were chosen based on the phase diagram of the Cu–As system [26]. Two samples with 30 at.% As and 60 at.% As composition were selected from the Cu₃As + As two-phase

region of the Cu-As phase diagram for the thermodynamic study of the low-temperature hexagonal modification of the Cu₃As compound (γ phase). For the study of the Cu₈As compound, samples with 15 at.% As and 20 at.% As composition were taken from the Cu₃As + Cu₈As

phase region, and for the examination of the solid solutions based on copper, the sample with 10 at.% As was selected from the Cu₈As + (Cu) phase area in the Cu-As phase diagram. Highpurity elements from Alfa-Aesar (copper rod, CAS number 7440-50-8, and arsenic pieces, CAS number 7440-38-2) were used for sample preparation.

Calculated amounts of elements were weighed on an analytical balance with ± 0.0001 g of accuracy before being put into quartz tubes. Tubes have been pumped to a pressure of 10^{-2} Pa and heated to the temperature of ~ 1150 K inside the muffle furnace. After the samples were melted for 3-4 hours at this temperature, they

were slowly cooled to 650 K during 5 hours and kept at the same temperature for ~500 hours. Later the samples were additionally annealed for ~100 hours at ~450K in order to adapt their condition closer to the temperature of *emf* measurements.

The PXRD technique was used to determine the phase composition of the prepared samples. Data collection was performed at room temperature using the D2 Phaser diffractometer with CuK $_{\alpha}$ emission. Samples were scanned from ~ 5 to 80°. The Topas 4.2 profile modeling software was used to examine and analyze the recorder diffraction patterns.

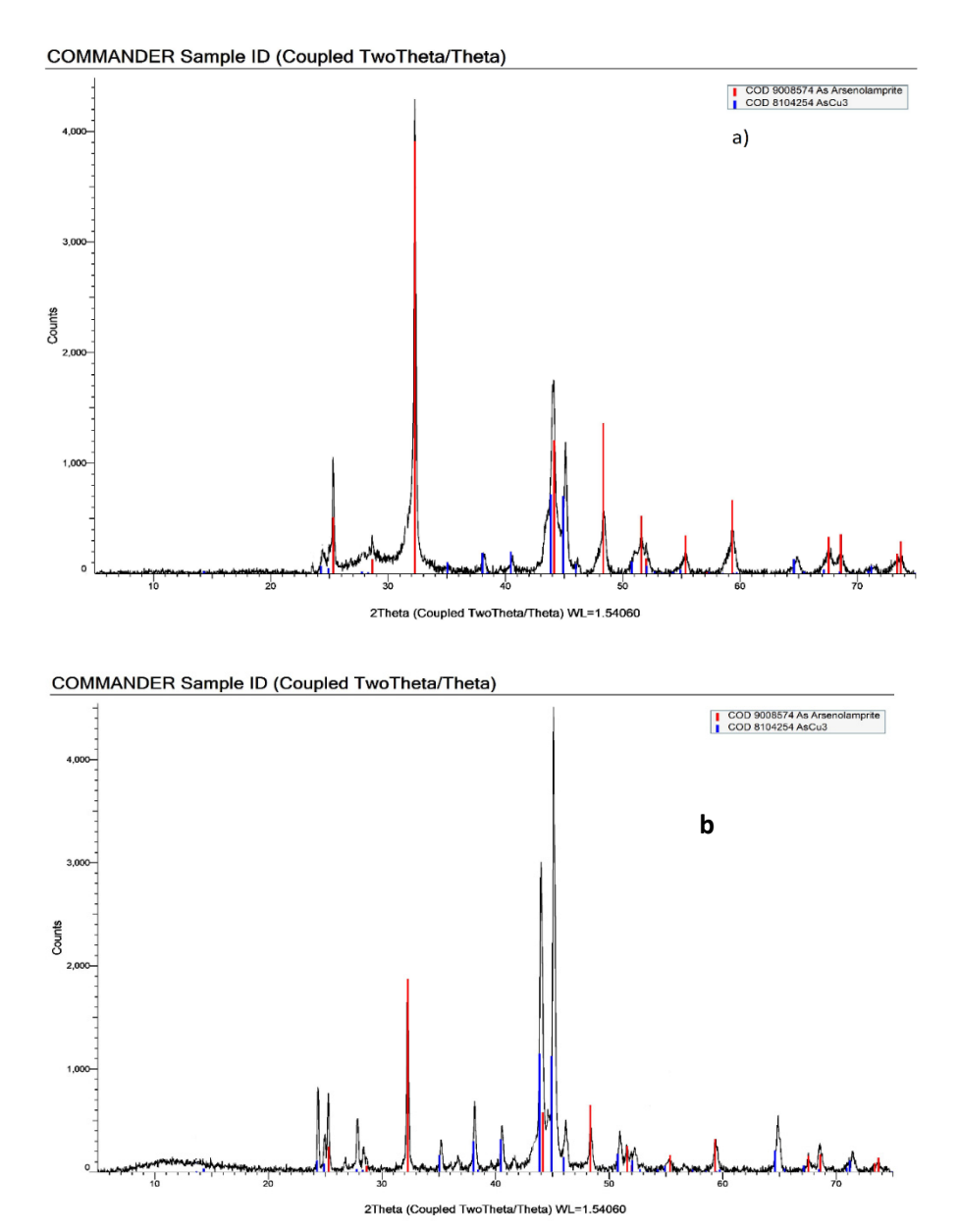


Fig. 2. Diffraction patterns of samples with a) 60 at. % As and b) 30 at. % As composition from the Cu₃As+As phase area in the Cu-As binary system

The PXRD patterns for selected 2 samples with 30 and 60 at.% As composition from the Cu₃As + As phase area are presented in Fig. 2. As shown, the X-ray diffractograms of both samples exhibit identical diffraction peaks corresponding to the low-temperature Cu₃As and As phases, albeit with varying intensities. No additional signals from other phases were detected, further confirming the successful

synthesis and complete homogenization of the samples. These PXRD results align with the expected phase composition, as outlined in the Cu-As phase diagram [25, 26], thereby validating the phase purity of the samples.

To start *emf* measurements, an electrochemical cell with the following sequence was constructed:

(-) Pt | Cu (solid) | Cu₄RbCl₃I₂ (solid electrolyte) | Cu₋As sample (solid) | Pt (+) (1)

The Cu4RbCl₃I₂ compound was employed as the solid electrolyte in cells of type (1). It was synthesized by melting stoichiometric amounts of reagent-grade anhydrous CuCl, CuI, and RbCl in an evacuated silica ampule at 900 K, followed by cooling to 450 K and thermal treatment at this temperature for approximately 100 hours. The resulting cylindrical ingot, approximately 0.6 cm in diameter, was then cut into pellets with a thickness of 0.3–0.4 cm, which were used as the solid electrolyte in the cells of type (1). Copper served as the left electrode, while pre-prepared equilibrium alloys of the Cu-As system were used as the right electrodes in cell (1).

Right electrodes were prepared using preliminarily synthesized and annealed alloys by powdering and pressing them into tablets having the same sizes as for solid electrolyte Cu₄RbCl₃I₂. The design of the electrochemical cell (1) and the *emf* measurements were carried out as outlined in [28, 33-36].

The digital multimeter Keithley 2100 6 $\frac{1}{2}$ having 1014 Ω input resistance and ± 0.1 mV accuracy was used to collect *emf* data in the 300-440 K temperatures interval. A chromel-alumel thermocouple and a mercury thermometer were used for temperature measurements. After keeping the cell at ~350 K for 40–60 hours, the first equilibrium values of the potential difference were obtained. Then subsequent measurements were taken every 3-4 h when a particular temperature was established. For equilibrium values of the *emf*, the difference between repeated measurements was not higher than 0.2 mV at the established temperature.

3. Results and discussions

Fig. 3 shows the dependence of the *emf* values of concentration cell of the type (1) on the composition along the Cu-As system at 300 K. Experimental measurements show that the *emf* values remain constant within each two-phase area, regardless of the overall composition of the electrode alloys, while changing sharply upon transition from one area to another. This confirms the phase equilibrium diagram of the Cu-As system [24-26] (Fig.1) and evidences a potential use of the *emf* measurements of the electrochemical cells (1) for thermodynamic calculations.

The temperature dependences of the *emf*

values for studied alloys in each phase area were found to be nearly linear (Fig. 4). This linear confirms stability behavior the of compositions of the coexisting phases in these regions over the studied temperature range. Additionally, it provides a basis for calculating the partial entropy and enthalpy using the temperature coefficients of the *emf* [36, 48]. This allowed to analyze the experimental E and T data by least-squares fitting using the Microsoft Office Excel software. The calculation procedure for the Cu₃As+As phase region is given in Table 1.

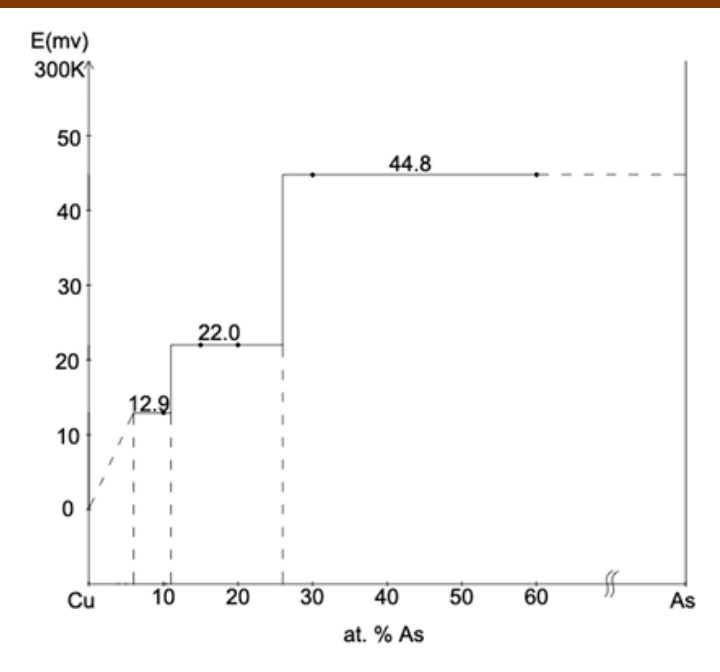


Fig. 3. The $E \sim f(x)$ dependences for the cells type (1) at 300 K

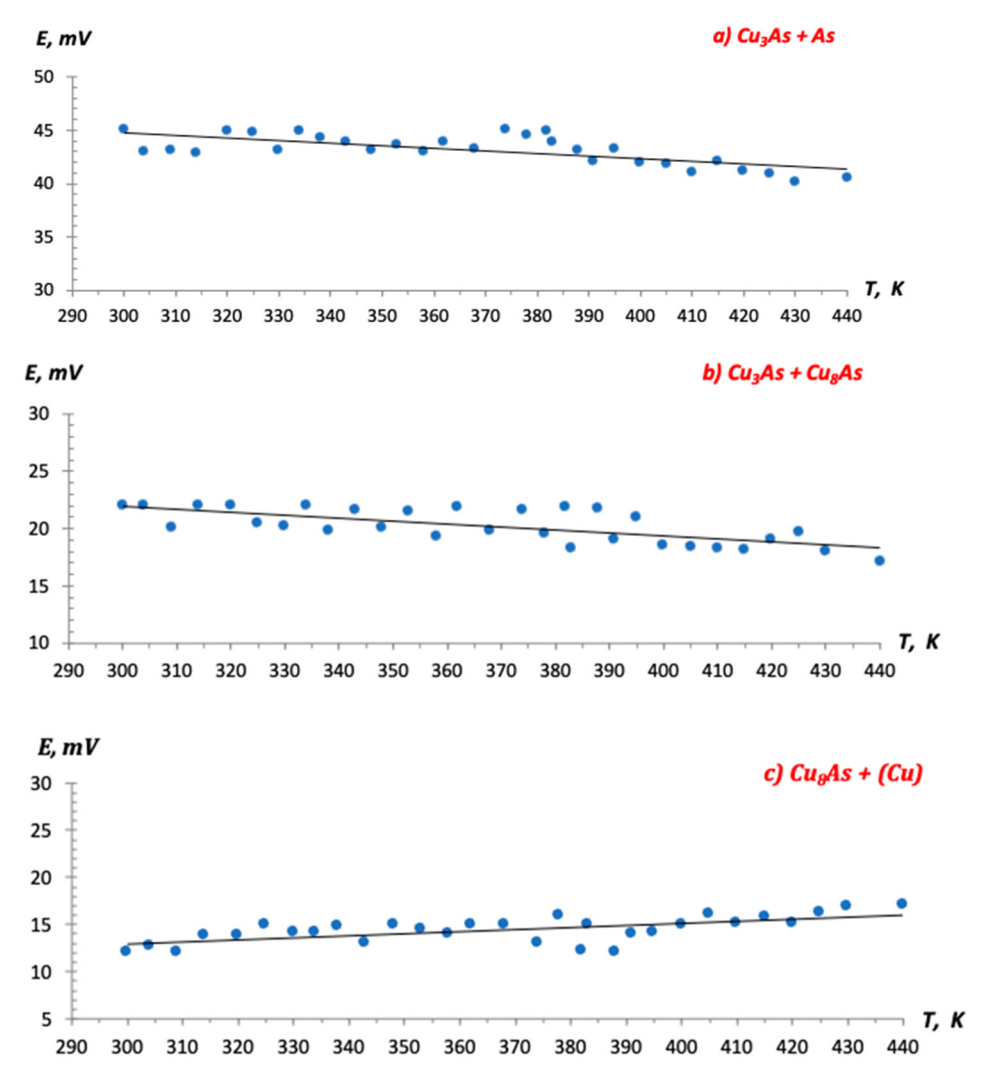


Fig. 4. $E \sim f(T)$ dependencies for the samples along the system Cu - As: (a) $Cu_3As + As$ phase area; (b) $Cu_3As + Cu_8As$ phase area; (c) $Cu_8As + (Cu)$ phase area

Table 1. Computer-processed *emf* measurement results for samples taken from the Cu₃As + As phase area

T_i, K	E_i, mV	$T_i - \overline{T}$	$E_i (T_i - \overline{T})$	$(T_i - \overline{T})^2$	Ĕ	$E_i - \widecheck{E}$	$(E_i - \overline{\overline{E}})^2$
300,0	45,00	-68,07	-3063,00	4633,07	44,76	0,24	0,06
304,0	43,00	-64,07	-2754,87	4104,54	44,67	-1,67	2,77
309,0	43,12	-59,07	-2546,95	3488,87	44,54	-1,42	2,03
314,0	42,79	-54,07	-2313,51	2923,20	44,42	-1,63	2,66
320,0	44,98	-48,07	-2162,04	2310,40	44,28	0,70	0,50
325,0	44,77	-43,07	-1928,09	1854,74	44,15	0,62	0,38
330,0	43,11	-38,07	-1641,05	1449,07	44,03	-0,92	0,85
334,0	44,88	-34,07	-1528,91	1160,54	43,94	0,94	0,89
338,0	44,22	-30,07	-1329,55	904,00	43,84	0,38	0,15
343,0	43,91	-25,07	-1100,68	628,34	43,72	0,19	0,04
348,0	43,17	-20,07	-866,28	402,67	43,59	-0,42	0,18
353,0	43,62	-15,07	-657,21	227,00	43,47	0,15	0,02
358,0	42,98	-10,07	-432,67	101,34	43,35	-0,37	0,14
362,0	43,88	-6,07	-266,21	36,80	43,25	0,63	0,39
368,0	43,27	-0,07	-2,88	0,00	43,11	0,16	0,03
374,0	44,99	5,93	266,94	35,20	42,96	2,03	4,11
378,0	44,55	9,93	442,53	98,67	42,86	1,69	2,84
382,0	44,90	13,93	625,61	194,14	42,77	2,13	4,55
383,0	43,88	14,93	655,27	223,00	42,74	1,14	1,29
388,0	43,14	19,93	859,92	397,34	42,62	0,52	0,27
391,0	42,08	22,93	965,03	525,94	42,55	-0,47	0,22
395,0	43,22	26,93	1164,06	725,40	42,45	0,77	0,59
400,0	42,00	31,93	1341,20	1019,74	42,33	-0,33	0,11
405,0	41,79	36,93	1543,44	1364,07	42,21	-0,42	0,17
410,0	41,04	41,93	1720,94	1758,40	42,09	-1,05	1,09
415,0	42,09	46,93	1975,42	2202,74	41,96	0,13	0,02
420,0	41,23	51,93	2141,21	2697,07	41,84	-0,61	0,38
425,0	40,91	56,93	2329,14	3241,40	41,72	-0,81	0,66
430,0	40,14	61,93	2486,00	3835,74	41,60	-1,46	2,13
440,0	40,54	71,93	2916,18	5174,40	41,36	-0,82	0,67
$\overline{T} = 368.067$	$\overline{E} = 43.107$		$\Sigma = -1160.98$	Σ = 47717.87			$\sum = 30.17$

Thus, analysis of the collected experimental data yields the linear equations of the following type:

$$E = a + bT \pm t \left[\frac{\delta_{\rm E}^2}{n} + \delta_{\rm b}^2 (T - \overline{T})^2 \right]^{1/2}$$
 (2)

where a and b are constant coefficients, n is the number of pairs of experimental E and T values; δ_E^2 and δ_b^2 are the error variances of the *emf* readings and b coefficient, respectively; \overline{T} is the average of the absolute temperature; t is Student's test. At a confidence level of 95% and a number of experimental points n=30, the

Student's criterion is $t=2.045 \approx 2.0$.

Obtained linear equations of the type (2) are presented in Table 2. Based on these linear equations and using the thermodynamic expressions below given, the partial molar thermodynamic functions of copper in alloys have been calculated [36, 47, 48]:

$$\Delta \overline{G}_{Cu} = -zFE \tag{3}$$

$$\Delta \overline{S}_{Cu} = zF \left(\frac{\partial E}{\partial T} \right)_P = zFb \tag{4}$$

$$\Delta \overline{H}_{Cu} = -zF \left[E - T \left(\frac{\partial E}{\partial T} \right)_P \right] = -zFa \tag{5}$$

where z is the number of electrons involved in J/mol). Obtained relative partial molar functions the reaction, and F is Faraday's constant (96,485 of copper in alloys are presented in Table 4.

Table 2. Linear equations obtained from the experimental data of the Cu-As system

Phase region	$E, mV = a + bT \pm 2S_E (T)$
Cu ₃ As + As	$52.06 - 0.0243 \text{ T} \pm 2 \left[\frac{1.01}{30} + 2.1 \cdot 10^{-5} (T - 368.07)^2 \right]^{1/2}$
$Cu_3As + Cu_8As$	$29.72 - 0.0259 \text{ T} \pm 2 \left[\frac{1.17}{30} + 2.4 \cdot 10^{-5} (T - 369.72)^2 \right]^{1/2}$
$(Cu) + Cu_8As$	$6.35 + 0.0219 \text{ T} \pm 2 \left[\frac{1.1}{30} + 2.3 \cdot 10^{-5} (T - 369.21)^2 \right]^{1/2}$

Table 3. Relative partial molar functions of copper in the alloys of the Cu-As system at 298K

Phase region	- ∆ \overline{G}_{Cu}	- ⊿ \overline{H}_{Cu}	$\Delta \overline{S}_{\mathrm{Cu}}$
	$kJ \cdot mol^{-1}$		$J \cdot mol^{-1} \cdot K^{-1}$
$Cu_3As + As$	4.32 ± 0.04	5.02 ± 0.16	-2.35 ± 0.44
Cu ₃ As + Cu ₈ As	2.12 ± 0.04	2.87 ± 0.18	-2.50 ± 0.48
$(Cu) + Cu_8As$	1.24 ± 0.04	0.61 ± 0.17	2.12 ± 0.46

Since the partial molar functions of copper for the Cu₃As compound correspond to the virtual reaction

$$Cu(s) + 1/3 As(s) = 1/3 Cu3As(s)$$
 (6)

thermodynamic functions of formula unit of this compound have been the standard formation and the standard entropy for one calculated based on the following expressions:

$$\Delta_f Z^0(Cu_3As) = 3 \cdot \Delta \overline{Z}_{Cu}$$

$$S^0(Cu_3As) = 3 \left[S^0(Cu) + \Delta \overline{S}_{Cu} \right] + S^0(As)$$
(8)

$$S^{0}(Cu_{3}As) = 3\left[S^{0}(Cu) + \Delta \overline{S_{Cu}}\right] + S^{0}(As)$$
 (8)

The virtual cell reactions for other two phases are given below:

$$5 \text{ Cu (s)} + \text{Cu}_3\text{As (s)} = \text{Cu}_8\text{As (s)}$$
 (9)
7.667 Cu (s) + Cu₈As (s) = 16.667 Cu_{0.94}As_{0.06} (s) (10)

The standard Gibbs free energy, enthalpy copper were calculated using the following and entropy of formation of the Cu₈As compound equations in accordance with the reactions (9) and the Cu_{0.94}As_{0.06} solid solutions based on the and (10):

$$\Delta_f Z^0(Cu_8 As) = 5 \Delta \overline{Z}_{Cu} + \Delta_f Z^0(Cu_3 As)$$
 (11)

$$\Delta_f Z^0(Cu_{0.94}As_{0.06}) = 0.46 \Delta \overline{Z}_{Cu} + 0.06 \Delta_f Z^0(Cu_8As)$$
 (12)

The absolute entropy was calculated according to the equations given below:

$$S^{0}(Cu_{8}As) = 5\left[S^{0}(Cu) + \Delta \overline{S_{Cu}}\right] + S^{0}(Cu_{3}As)$$
(13)

$$S^{0}(Cu_{0.94}As_{0.06}) = 0.46 \left[S^{0}(Cu) + \Delta \overline{S_{Cu}} \right] + 0.06 S^{0}(Cu_{8}As)$$
 (14)

Errors were calculated by the error accumulation method. Absolute entropies of the elementary copper and arsenic used for calculations were taken from [49]: $S^0(Cu) =$

 33.15 ± 0.08 J/(mole · K); $S^0(As) = 35.61 \pm 0.04$ J/(mole · K). Calculated standard integral thermodynamic functions including available literature data are summarized in Table 4.

Table 4. Standard integral thermodynamic functions of copper arsenides

Compound	$-\Delta_{\mathbf{f}}\mathbf{G}^{0}$	$-\Delta_{\mathbf{f}}\mathbf{H}^{0}$	$\Delta_{\mathbf{f}} \mathbf{S}^{0}$	S^0	Reference,	
	kJ · mol⁻¹		$J \cdot mol^{-1} \cdot K^{-1}$		method	
Cu ₃ As	12.96±0.12	15.06±0.48	-7.04±1.32	128.0±1.6	This work, <i>emf</i>	
		11.715			[49], recomm.	
		11.7		137.2	[50], recomm.	
		11.7			[51], recomm.	
		10.7			[52], recomm.	
		75.8			[53], evaluation	
		15.0			[54], evaluation	
	69.0	14.634	182		[55], vapor press.	
		14.6 ± 3.8			[56], calorimetry	
		17.9 ± 2.9		126.7	[57], calorimetry	
Cu ₈ As	23.56±0.32	29.41±1.38	-19.62±3.72	281.3±4.4	This work, <i>emf</i>	
Cu _{0.94} As _{0.06}	1.98±0.05	2.05±0.16	0.23±0.44	33.3±0.5	This work, <i>emf</i>	

As shown in Table 4, the standard formation enthalpies (ΔfH⁰) of the Cu₃As compound have been calculated and reported by various authors, with values differing between studies. The results from the present work show a closer agreement with those derived from calorimetric and vapor pressure measurements [54-57]. In contrast, the $\Delta_f H^0$ values found in the handbooks and reference works [49-51] are lower, likely sourced from older data. Given that pressure the calorimetric and vapor measurements are more recent, they provide a representation accurate thermodynamic properties of Cu₃As.

Furthermore, this study represents the first

determination of the standard integral thermodynamic functions and absolute entropy for the Cu₈As compound and the Cu_{0.94}As_{0.06} solid solutions. The data presented herein helps resolve some of the inconsistencies in the literature regarding the thermodynamics of the Cu₃As compound. We believe that our findings significantly advance the understanding of copper arsenides' thermodynamic properties and will be valuable for future thermodynamic calculations. These results can be incorporated various handbooks and databases. comprehensive contributing to a more understanding of the behavior and stability of copper arsenide materials.

4. Conclusion

In this study, we present the results of a thermodynamic investigation of copper arsenides using the low-temperature *emf* method with a solid Cu⁺ conductive electrolyte, Cu₄RbCl₃I₂, conducted within a temperature range of 300 to 440 K. By employing samples from the Cu₃As + As, Cu₃As + Cu₈As, and Cu₈As + (Cu) two-phase regions as the right electrodes, linear equations describing the temperature dependence of the

emf were derived. From these equations, the partial molar thermodynamic functions of copper in alloys were calculated. Potential-generating reactions for the studied intermediate phases were identified using the T-x diagram of the Cu-As system, enabling the determination of their standard integral thermodynamic functions. Presented mutually consistent thermodynamic values are the first experimental data derived

from the *emf* measurements near standard conditions. These standard thermodynamic values are highly precise and contribute

significantly to the understanding of copper arsenides' thermodynamics, helping to reconcile discrepancies in the existing literature.

References

- 1. Enescu D. Innovations in Thermoelectric Technology: From Materials to Applications. *Energies*. 2024, **vol. 17(7)**, p. 1692. https://doi.org/10.3390/en17071692
- Bortnikova S., Bessonova E., Gaskova O. Geochemistry of arsenic and metals in stored tailings of a Co–Ni arsenide-ore, Khovu-Aksy area, Russia. *Applied Geochemistry*. 2012, vol. 27(11), p. 2238-2250. https://doi.org/10.1016/j.apgeochem.2012.02.033
- 3. Raabe D. The materials science behind sustainable metals and alloys. *Chemical reviews*. 2023, vol. 123(5), p. 2436-2608. https://doi.org/10.1021/acs.chemrev.2c00799
- 4. Hu Y., Liang J., Xia Y., Zhao C., Jiang M., Ma J., Tie Z., Jin Z. 2D Arsenene and Arsenic Materials: Fundamental Properties, Preparation, and Applications. *Small.* 2022, vol. 18(9), p. 2104556. https://doi.org/10.1002/smll.20210 4556
- Buschow K.H.J., Cahn R.W. Encyclopedia of materials: science and technology. 2001, 2nd ed. https://doi.org/10.1016/B978-0-08-043152-9.X5000-1
- 6. Vurgaftman I., Meyer J.A.R., Ram-Mohan L.R. Band parameters for III–V compound semiconductors and their alloys. *Journal of applied physics*. 2001, **vol. 89(11)**, p. 5815–5875. https://doi.org/10.1063/1.1368156
- 7. Sze S.M., Ng K.K. *LEDs and lasers. Physics of semiconductor devices*. 2006, vol. 3, p. 601–657.
- Sharma R.C., Nandal R., Tanwar N., Yadav R., Bhardwaj J., Verma A. Gallium arsenide and gallium nitride semiconductors for power and optoelectronics devices applications. In *Journal of Physics: Conference Series*. 2023, vol. 2426(1), p. 012008. https://doi.org/10.1088/1742-6596/2426/1/012008
- 9. Ali A., Anwar A.W., Moin M., Babar M., Thumu U. Investigation of structural, mechanical, electronic and optical responses of Ga doped aluminum arsenide for

- optoelectronic applications: By first principles. *Heliyon*. 2024, **vol. 10(2)**. https://doi.org/10.1016/j.heliyon.2024.e2459
- 10. Colombo C., Heiβ M., Grätzel M., Fontcuberta i Morral A. Gallium arsenide pin radial structures for photovoltaic applications. *Applied Physics Letters*. 2009, **vol**. 94(17). https://doi.org/10.1063/1.3125435
- 11. Islam M.M., Kauzlarich S.M. The Potential of Arsenic-based Zintl Phases as Thermoelectric Materials: Structure & Thermoelectric Properties. Zeitschrift für anorganische und allgemeine Chemie. 2023, **vol.** 649(21), e202300149. https://doi.org/10.1002/zaac.202300149
- 12. Giurlani W., Pappaianni G., Bonechi M., Calisi N., Mannini M., Bazzicalupi C. Innocenti M. Electrodeposition of Manganese Arsenides (Mn_xAs) as Promising Candidates in Spintronics. In *Electrochemical* Meeting Society Abstracts. 2023, vol. 243(22), p. 1554-1554. https://doi.org/10.1149/MA2023-01221554mtgabs
- 13. Kim S., Yeon S., Lee M., Jin J., Shin S., Gwak N., Oh N. Chemically and electronically active metal ions on InAs quantum dots for infrared detectors. *NPG Asia Materials*, 2023, 15, 30. https://doi.org/10.1038/s41427-023-00477-w
- 14. Zhang C., Narayan A., Lu S., Zhang J., Zhang H., Ni, Z., Xiu F. Evolution of Weyl orbit and quantum Hall effect in Dirac semimetal Cd₃As₂. *Nature communications*. 2017, vol. 8(1), p.1272. https://doi.org/10.1038/s41467-017-01438-y
- 15. Jia Z., Li C., Li X., Shi J., Liao Z., Yu D., Wu X. Thermoelectric signature of the chiral anomaly in Cd₃As₂. *Nature communications*. 2016, vol.7(1), p.13013. https://doi.org/10.1038/ncomms13013
- 16. Shishin D., Hidayat T., Jak E., Decterov S., Belov G.V. Thermodynamic database for

- pyrometallurgical copper extraction. In *Proc.: Copper.* 2016, **vol. 1805**, p. 12. https://doi.org/10.1063/1.4974425
- 17. Chen C., Zhang L., Jahanshahi S. Thermodynamic modeling of arsenic in copper smelting processes. *Metallurgical and Materials transactions B.* 2010, vol. 41(6), p.1175-1185. https://doi.org/10.1007/s11663-010-9431-z
- 18. Chaubal P.C., Nagamori M. Thermodynamics for arsenic and antimony in copper matte converting—computer simulation. *Metallurgical Transactions B*. 1988, **vol.** 19, p. 547-556. https://doi.org/10.1007/BF02659145
- 19. Prostakova V., Shishin D., Jak E. Thermodynamic optimization of the Cu–As–S system. *Calphad*. 2021, **vol 72**, p. 102247. https://doi.org/10.1016/j.calphad.2020.1022
- 20. Hansen M., Anderko K. Constitution of Binary Alloys. *2nd Ed., Metallurgy and Metallurgical Engineering Series*. Published by McGraw-Hill Book Co., New York City, 1958. 1305 p.
- 21. Elliot R. Constitution of Binary Alloys, First Supplement, McGraw-Hill, New York.1965
- 22. Juza R., von Benda K. Zur Kenntnis des "Cu₅As₂". *Zeitschrift für anorganische und allgemeine Chemie*. 1968, **vol. 357(4-6)**, p.238-246. https://doi.org/10.1002/zaac.19683570411
- 23. Naud J., Priest P. Study on copper-arsenic system. *Materials Research Bulletin*. 1972, vol. 7(8), p. 783.
- 24. Subramanian P.R., Laughlin D.E. The As—Cu (arsenic-copper) system. *Bulletin of Alloy Phase Diagrams*. 1988, **vol. 9(5)**, p.605-618. https://doi.org/10.1007/BF02881964
- 25. Taskinen P., Teppo O. An Assessment of the Thermodynamic Properties of Arsenic-Copper Alloys. *Scandinavian Journal of Metallurgy*. 1991, vol. 20(3), p.141-148.
- 26. Shishin D., Jak E. Critical assessment and thermodynamic modeling of the Cu-As system. *Calphad*. 2018, **vol. 60**, p. 134-143. https://doi.org/10.1016/j.calphad.2017.12.00
- 27. Vassiliev V.P., Gong W. Electrochemical Cells-New Advances in Fundamental Research and Applications. 2012, *chapter*, *4*, p. 71-102. https://doi.org/10.5772/39007

- 28. Shao Y. Electrochemical Cells New Advances in Fundamental Research and Applications, 2012, 10.5772/1890, Chapter 5. https://doi.org/10.5772/39007
- 29. Tesfaye F., Taskinen P. Experimental thermodynamic study of the equilibrium phase AgBi₃S₅ by an improved EMF method. *Thermochimica Acta*. 2013, **vol.** 562, p.75-83. https://doi.org/10.1016/j.tca.2013.03.011
- 30. Katayama I., Shimazawa K., Živković D., Manasijević D., Živković Ž., Iida T. Activity measurements of Ga in liquid Ga–Tl alloys by EMF method with zirconia solid electrolyte. *International Journal of Materials Research*. 2022, vol. 94(12), p.1296-1299. https://doi.org/10.1515/ijmr-2003-0234
- 31. Babanly D.M., Aghayeva A.R., Mammadova S.H., Tagiyev D.B. Thermodynamic study of the CdSb compound by the electromotive force measurements method. *Chemical Problems*. 2024, vol. 22(4), p. 402-410. DOI: 10.32737/2221-8688-2024-4-402-410
- 32. Aghayeva A.R., Babanly D.M., Mammadova S.H., Djafarov Y.I., **Tagiyev** D.B. Thermodynamic Study of Zinc Antimonides by the electromotive force measurements. Condensed Matter and Interphases. 2025, vol. 27(1), 48-56 p. https://doi.org/10.17308/kcmf.2025.27/1248
- 33. Mammadli P.R., Mashadiyeva L.F., Hasanova Z.T., Babanly D.M. Thermodynamic study of a synthetic analog of the famatinite mineral- Cu₃SbS₄. *Physics and Chemistry of Solid State*. 2021, **vol. 22(1)**, p. 53-58. https://doi.org/10.15330/pcss.22.1.53-58
- 34. Babanly M.B., Mashadiyeva L.F., Imamaliyeva S.Z., Tagiev D.B., Babanly Yusibov Thermodynamic D.M., Y.A. properties of complex copper chalcogenides review. Chemical Problems. 2024. vol. 22(3), 243-280. p. https://chemprob.org/wpcontent/uploads/2024/05/243-280.pdf
- 35. Babanly M.B., Yusibov Y.A. Elm, Baku, 2011. in Russian.
- 36. Babanly M.B., Yusibov Y.A, Babanly N.B. Ed. S.Kara. Intechweb.Org. 2011. p.57-78.

- 37. Babanly N.B., Salimov Z.E., Akhmedov M.M., Babanly M.B. Thermodynamic study of Cu-Tl-Te system using EMF technique with Cu₄RbCl₃I₂ solid electrolyte. *Russian Journal of Electrochemistry*. 2012, **vol.** 48, p. 68-73.
 - https://doi.org/10.1134/S102319351201004
- 38. Mashadiyeva L.F., Mammadli P.M., Babanly D.M., Ashirov G.M., Shevelkov A.V., Yusibov Y.A. Solid-Phase Equilibria in the Cu-Sb-S System and Thermodynamic Properties of Copper-Antimony Sulfides. *JOM.* 2021, **vol.** 73(5), p.1522-1530. doi:10.1007/s11837-021-04624-y
- 39. Ivanov Shchits A.K., Murin I.V. Ionika tverdogo tela (Ionics of Solids), *Izdvo SPbGU*. 2000, vol. 1.
- 40. Gurevich Yu.Ya., Kharkats Yu.I. Superionnye provodniki (Superionic Conductors), Moscow. 1992.
- 41. Babanly M.B., Gasanova Z.T., Mashadieva L.F., Zlomanov V.P., Yusibov Y.A. Thermodynamic study of the Cu-As-S system by EMF measurements with Cu₄RbCl₃I₂ as a solid electrolyte. *Inorganic Materials*. 2012, **vol.** 48(3), p. 225-228. https://doi.org/10.1134/S002016851202002
- 42. Babanly N. B., Aliev Z. S., Yusibov Y. A., Babanly M. B. A thermodynamic study of Cu—Tl—S system by EMF method with Cu4RbCl3I2 solid electrolyte. *Russian Journal of Electrochemistry*. 2010, 46(3), p. 354-358.
 - DOI: 10.1134/S1023193510030146
- 43. Alverdiev I.J., Abbasova V.A., Yusibov **Tagiev** D.B., Babanly Thermodynamic Study of Cu₂GeS₃ and Cu₂xAgxGeS3 Solid Solutions by the EMF Method with Cu₄RbCl₃I₂ Solid a Electrolyte. Russian Journal of Electrochemistry. 2018, vol. 54, p. 195-200. https://doi.org/10.1134/S102319351802002
- 44. Mashadieva L.F., Gasanova Z.T., Yusibov Y.A., Babanly M.B. Phase Equilibria in the Cu₂Se–Cu₃AsSe₄–Se System and Thermodynamic Properties of Cu₃AsSe₄. *Inorganic Materials*. 2018, vol. 54, p. 8-16.

- https://doi.org/10.1134/S002016851801009
- 45. Babanly N.B., Yusibov Y.A., Mirzoeva R.J., Shykhyev Y.M., Babanly M.B. Cu₄RbCl₃I₂ solid superionic conductor in thermodynamic study of three-component copper chalcogenides. *Russian Journal of Electrochemistry*. 2009, vol. 45, p. 405-410. https://doi.org/10.1134/S102319350904008
- 46. Babanly D.M., Aghayeva A.R., Mirzayev R.E., Mashadiyeva L.F., Djafarov Ya.I. Thermodynamic Study of Copper Antimonides by the EMF Method with the Cu₄RbCl₃I₂ Solid Electrolyte. *Russ. J. Phys. Chem.* 2024, **vol.** 98, p. 3266–3272. https://doi.org/10.1134/S0036024424702777777
- 47. Moroz M., Demchenko P., Prokhorenko M., Reshetnyak O., Tesfaye F. Phase Equilibria and Thermodynamic Properties of Compounds in the Ag₂FeS₂—Ga₂S₃ Cross-Section of the Ag–Fe–Ga–S System Determined by the EMF Method. *JOM*. 2024, p. 1-8. https://doi.org/10.1007/s11837-024-07024-0
- 48. Morachevsky A., Voronin G., Geyderich V., Kutsenok I. *Akademkniga Publ.* Moscow: p. 334. 2003. Available at https://elibrary.ru/item.asp?id=19603291.
- 49. Iorish V.S., Yungman V.S. *Thermal constants of substances*. 2006, Database.
- 50. Barin I. *Thermochemical data of pure substances* (3rd ed.). 2008, Wiley-VCH.
- 51. Wagman D.D, Evans W.H., Parker V.B., Schumm R.H., Halo I., Bailey S.M., Chutney L.L., Neutral J. Table 36: Copper. In *Selected Values of Chemical Thermodynamic Properties*, National Bureau of Standards (NBS), Washington, D.C, 1967.
- 52. Weibke F., Kubaschewski O. *Thermochemie der legierungen. 2013*, vol. 10. Springer-Verlag.
- 53. Nagamori M. Thermodynamic behaviour of arsenic and antimony in copper matte smelting-a novel mathematical synthesis. *Canadian metallurgical quarterly*. 2001, vol. 40(4), p. 499-522. https://doi.org/10.1179/cmq.2001.40.4.499
- 54. Shishin D., Jak E. Critical assessment and thermodynamic modeling of the Cu-As system. *Calphad*. 2018, **vol. 60**, p. 134-143.

- https://doi.org/10.1016/j.calphad.2017.12.00
- 55. Wypartowicz J. Thermodynamic properties of copper-arsenic liquid solutions. *Journal of alloys and compounds*. 1995, vol. 227(1), p.86-92. https://doi.org/10.1016/0925-8388(95)01639-2
- 56. Wypartowicz J., Fitzner K., Kleppa O. J. Standard enthalpy of formation of Cu₃As and heats of mixing in the liquid systems CuAs and FeAs by direct combination high
- temperature drop calorimetry. *Journal of alloys and compounds*. 1995, **vol. 217(1)**, p. 1-4. https://doi.org/10.1016/0925-8388(94)01287-R
- 57. Espeleta A.K., Yamaguchi Itagaki K., Shigen-toSozai. Calorimetric Study of Some Arsenides and Antimonides (MxAsy and MxSby (M=Cu,Fe,Co,Ni)). *Shigen Sozai*. 1991, vol. 107(9), p. 658–663. https://doi:10.2473/shigentosozai.107.658